Progress Report, 2005, Southern California Earthquake Center

Thermal Weakening in Large Seismic Slips and Effects on Rupture Dynamics

James R. Rice (PI), Harvard University, Cambridge, MA 02138
19 November 2005

Recent reports related to theme of this project:

Abercrombie, R. E., and J. R. Rice (2005), "Can observations of earthquake scaling constrain slip weakening?", *Geophysical Journal International*, **162**, pp. 406–424, doi: 10.1111/j.1365-246X.2005.02579.x. http://esag.harvard.edu/rice/212_AbercrombieRice_GJI05.pdf

Rice, J. R. (2005), "Heating and weakening of faults during earthquake slip", manuscript submitted to *Journal of Geophysical Research*. http://esag.harvard.edu/rice/Rice_heat_weaken_toJGR05.pdf

Rice, J. R. (2005), "Mechanical role of fluids in earthquakes and faulting", *Eos Trans. AGU, 86*(52), Fall Meet. Suppl., Abstract T43C-03.

Rice, J. R., and M. Cocco (2005), "Seismic fault rheology and earthquake dynamics", in *The Dynamics of Fault Zones*, ed. M. R. Handy, Dahlem Workshop (Berlin, January 2005) Report 95, The MIT Press, Cambridge, MA, USA, publication expected 2006. http://esag.harvard.edu/rice/216_RiceCocco_DahlemWrkshp05.pdf

Rice, J. R., J. W. Rudnicki, and V. C. Tsai (2005), "Shear localization in fluid-saturated fault gouge by instability of spatially uniform, adiabatic, undrained shear", *Eos Trans. AGU, 86*(52), Fall Meet. Suppl., Abstract T13E-05.

Rice, J. R., C. G. Sammis and R. Parsons (2005), "Off-fault secondary failure induced by a dynamic slip-pulse", *Bulletin of the Seismological Society of America*, 95(1), pp. 109–134, doi: 10.1785/0120030166. http://esag.harvard.edu/rice/211_RiceSammisPars_BSSA05.pdf

Rudnicki, J. W., and J. R. Rice (2005), "Effective normal stress alteration during earthquakes due to pore pressure induced by contrasting properties bounding the rupture plane", *Eos Trans. AGU, 86*(52), Fall Meet. Suppl., Abstract T13E-04.

Xia, K., A. J. Rosakis, H. Kanamori and J. R. Rice (2005), "Laboratory earthquakes along inhomogeneous faults: Directionality and supershear", *Science*, 308 (5722), pp. 681-684. http://esag.harvard.edu/rice/ 215_XiaRosKanRi_bimat_Sci05.pdf

Progress:

The research seeks to understand the physical basis for weakening of fault zone shear resistance during seismic slip.

(1) A major result has been to show the plausibility that two major thermal weakening processes might dominate at least the early phases of earthquake fault zone response during seismic slip [Rice, 2005; Rice and Coco, 2005]. Those are flash heating at frictional micro-asperity contacts, and thermal pressurization of pore fluid within the granulated and porous ultracataclastic core of a mature fault. A simple representation of these effects has been devised for slip on a plane, at constant slip rate V, with constant friction coefficient f, in which case the solution, when we linearize the differential equations expressing conservation of energy and pore fluid mass, is $\tau = f(\sigma_n - p) = f(\sigma_n - p_o)\exp\left(\delta / L^*\right)\mathrm{erfc}\left(\sqrt{\delta / L^*}\right)$ (plotted in Figure 1).

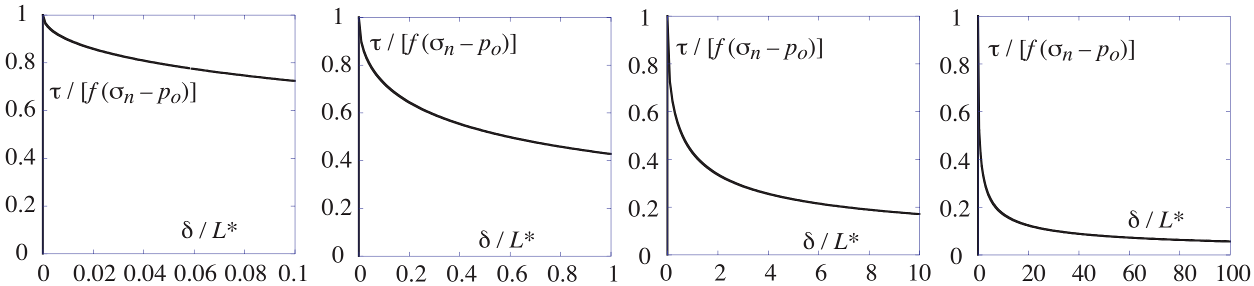

Figure 1 [Rice, 2005]: Prediction of shear strength τ versus slip δ, due to *thermal pressurization of pore fluid* during slip on a plane, at constant rate *V* and with constant friction coefficient *f*, in a fluid-saturated solid. Note the apparent multiscale nature of the weakening, although there is a single *L**.

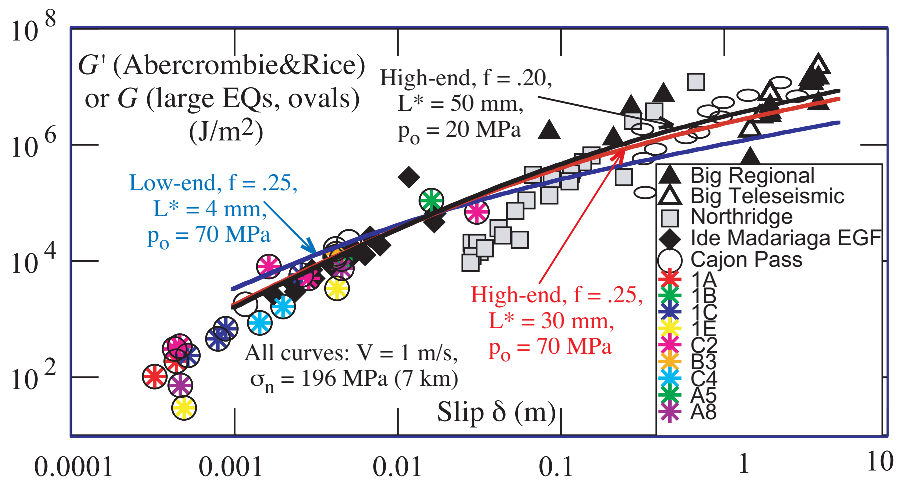

Figure 2 [Rice, 2005]: Lines show theoretical predictions of earthquake fracture energy *G* versus slip δ in the event, for the model of slip on a plane, based on combined effects of *thermal pressurization* of pore fluid and *flash heating*, with simplified representation assuming a constant friction coefficient *f* and slip rate *V*. The combination $f^2\ V\ L^*$ depends only on thermo-poro-mechanical properties assumed for the fault gouge, and is different for the models designated "low end" (based on lab-estimated intact properties corresponding to 7 km depth) and "high end" (accounting for damage and permeability increase at the rupture front). *A new addition, over a similar plot shown last year, is that estimates of G have now been added for 12 large earthquakes. Those are based on processing results of finite-source seismic slip inversions by the method of one or both of Rice, Sammis, and Parsons [2005] and/or Tinti, Spudich and Cocco [JGR, 2005]; those new results are represented by the 12 oval symbols in the upper right.*

Here σ_n is fault-normal stress and p_o is the pore pressure just after its reduction from ambient pressure by dilatancy at onset of shear. Also, the length parameter *L** which enters is defined by $f^2 V L^* = 4\left(\rho c / \Lambda\right)^2 \left(\sqrt{\alpha_{hy}} + \sqrt{\alpha_{th}}\right)^2$, where α_{th} and α_{hy} are the thermal and hydraulic diffusivities, ρc is the specific heat per unit mass, and Λ is the poroelastic parameter giving *dp/dT* under undrained heating at constant normal stress. Using permeability and poroelastic data [Wibberley and Shimamoto, 2003] for the gouge of the central slip zone of the Median Tectonic

Line fault in Japan, and the thermophysical properties of water and rock, it was estimated [Rice, 2005] that at a representative centroidal depth of crustal rupture, $(\rho c / \Lambda)^2 \left(\sqrt{\alpha_{hy}} + \sqrt{\alpha_{th}}\right)^2 \approx$ $65\ \text{mm}^2/\text{s}$ if there is intact elastic response of the fault wall gouge (referred to as the "low-end" parameter choice), and $\approx 470\ \text{mm}^2/\text{s}$ if we account very approximately for increased permeability and compressibility of the gouge due to damage imparted to it at the rupture front (the "high-end" parameter choice). For $V = 1$ m/s and $f = 0.25$ (reduced by flash heating [Tullis and Goldsby, 2003; Prakash, 2004]), that means $L^* \approx 4$ mm based on intact properties and 30 mm based on damaged.

The corresponding fracture energy is

$$G(\delta) = \int_0^\delta [\tau(\delta') - \tau(\delta)]d\delta' = f(\sigma_n - p_o)L^* \left[\exp\left(\frac{\delta}{L^*}\right)\text{erfc}\left(\sqrt{\frac{\delta}{L^*}}\right)\left(1 - \frac{\delta}{L^*}\right) - 1 + 2\sqrt{\frac{\delta}{\pi L^*}} \right],$$

and that is compared to estimates of G from seismic data in Figure 2 (see further discussion in the companion proposal for 2006).

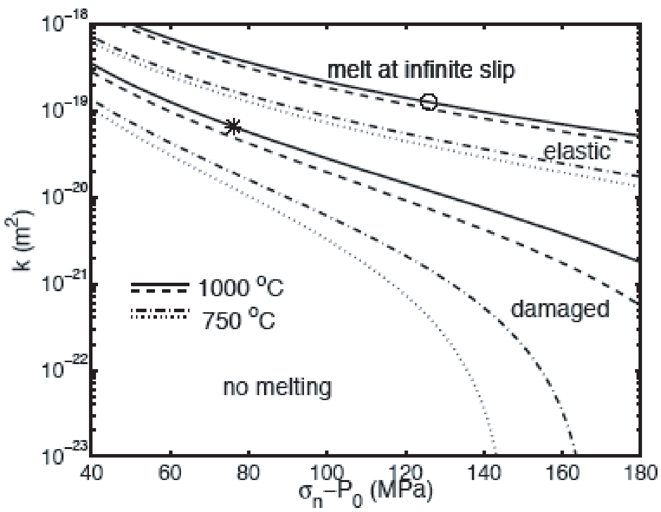

Figure 3 [Rempel and Rice, 2005, in progress]: Regime diagram showing the permeability as a function of initial effective stress required for melting conditions to be reached in a finite amount of slip. The upper two pairs of curves were calculated assuming intact elastic gouge behavior (low-end parameter choice). Solid and dashed curves are for an assumed melt onset of 1000 C; dot-dashed and dotted for a melt onset of 750 C. The lower two pairs of curves show the corresponding calculations assuming damaged fault walls (high end parameters). Each curve divides a region above it, in which melt onset will occur at some sufficiently large slip, from a region below it for which melting never occurs, no matter how large the slip.

(2) In work in progress, now at the stage of a semi-final draft of a manuscript on thermal pressurization and onset of melting in fault zones, former postdoc A. W. Rempel and Rice have evaluated thermophysical properties of gouge and pore water with the aim of defining conditions under which the onset of melting would begin despite the reduced rate of temperature rise due to the thermal pressurization mechanism. That works adopts the model of a very thin, possibly sub-mm, but nevertheless finite thickness of the shearing zone. Then, for small slip distances, heat and pore fluid are unable to escape the shearing fault core and the behavior is well approximated by simple analytical models that neglect any transport. Following larger slip distances, the finite width of the shear zone is small compared to the thicknesses of the thermal and hydrological boundary layers, and the fault behavior approaches that predicted as above for the idealized case of slip on a plane. To evaluate the range in which the predictions of these two sets of approximations are valid, we developed a model that describes how frictional dissipation within a finite shear-zone drives heat and mass transport through the surrounding static gouge. With realistic parameter values and slips greater than a few cm, the subsequent evolution of strength and fracture energy are approximated well by the planar-slip model. However, the temperature evolution is much more sensitive to the finite shear zone thickness, and the ultimate temperature rise tends to be intermediate between that predicted for the two simplified cases. We explore the range of conditions necessary for melting to begin (e.g., Figure 3) and focus in particular on the potential role of fault-zone damage in facilitating fluid transport and promoting larger temperature increases. We discuss how the apparent scarcity of exhumed pseudotachylytes places constraints on some of the more uncertain fault-zone parameters.

(3) In closely related work, we have also shown how the presence of pore fluids in gouge, together with their shear heating in rapid frictional deformation, promotes extreme shear localization [Rice, Rudnicki and Tsai, 2005]. We examined the dynamics of a shear zone of fluid-saturated gouge under homogenous, undrained, adiabatic shear, and showed that such deformation is unstable, in a manner that suggests strong shear localization. The material is assumed to follow the Coulomb friction law but to be rate-strengthening, such that its friction coefficient increases with shear strain rate $\dot{\gamma}$ (if rate-weakening, deformation would localize at the onset of shear). This rate-strengthening model is of interest because it applies to stable regions in which rupture cannot nucleate and to initially unstable regions that have been driven into a stable temperature regime by shear heating. This shearing has been shown in our work to be linearly unstable in the sense that small perturbations from uniform shearing result in exponential growth for all wavelengths greater than a critical wavelength. Setting the shear zone width equal to this critical wavelength, provides a rough estimate of the largest width *h* over which such uniform shearing is stable. That is given by $h = 4\pi^2(\alpha_{th} + \alpha_{hy})\rho c / [(z+2)\Lambda V]$ where *V* is the net slip rate across the shear zone, and $1/z = (\dot{\gamma} df / d\dot{\gamma})/f$ is a measure of the strengthening of friction coefficient *f* with $\dot{\gamma}$. Choosing *z* = 40 (z ~20-60 based on known lab experiments showing rate strengthening, unfortunately all done at low $\dot{\gamma}$), average earthquake slip rate *V* = 1 m/s, and values [Rice, 2005] $\alpha_{th} = 0.7\ \text{mm}^2/\text{s}$, $\alpha_{hy} = 4\ \text{mm}^2/\text{s}$, and $\Lambda / \rho c = 0.1$, thought to be relevant to deforming ultracataclastic gouge at typical centroidal depths of the crustal seismogenic zone, we estimate $h \approx 0.04$ mm. This mechanism, therefore, may help explain the field observation of sub-millimeter-sized high shear zones [Chester et al., 2003] within a much thicker gouge layer. Graduate student Victor Tsai (independently supported) is also performing a more detailed, numerical analysis that takes into account nonlinearities and pressure and temperature dependencies of the shear zone poromechanical properties, to more accurately describe the dynamics within the shear zone. The results thus far demonstrate the approximate validity of the linear stability analysis, including the above prediction of the localized zone thickness, which strictly lies beyond the range of its applicability.

(4) We have identified a new mechanism [Rudnicki and Rice, 2001] by which dissimilarity, between the two sides of the fault, in permeability and poroelastic properties within the fringes of damaged, granulated gouge immediately bordering the slip surface, say, over a scale of a few 10's to perhaps 100's of mm, can significantly alter effective normal stress during slip. This involves an alteration of pore pressure. The effect is complementary to the Weertman [*JGR*, 1980] effect, much studied by Andrews and Ben-Zion [1997] and Harris and Day [1997], by which dissimilarity of elastic properties and density can alter the total normal stress during slip. Both have in common that their effect on effective stress reverses when the materials are switched, for a given direction of rupture propagation, or when the direction of propagation is switched for a given set of materials. Thus either effect can be positive or negative, depending on the contrast in properties, and the two effects can augment or offset each other.

The effect is most readily illustrated by considering, like in Weertman [1980], a pulse of mode II slip which moves in steady state, at propagation speed v, along the x axis, which is the interface between the dissimilar materials. Thus the slip $\delta = \delta(x - \mathrm{v}t)$, and if superscript "0" denotes stresses or pore pressure before the rupture appears, then the Weertman equations are modified to:

$$\sigma_{xy}(x) = \sigma_{xy}^0 - \frac{\bar{\mu}(\mathrm{v})}{\pi} \int_{-\infty}^{+\infty} \frac{d\delta(x')/dx'}{x - x'} dx'$$

$$\sigma_{yy}(x) + p(x) = (\sigma_{yy}^0 + p^0) - \left(\mu^*(\mathrm{v}) + \frac{W(\mathrm{v})}{2}\right) \frac{d\delta(x)}{dx}$$

In fact, the first is unchanged and $\bar{\mu}(\mathrm{v})$ is Weertman's well known function which vanishes at the generalized Rayleigh speed. However, the second equation now refers to the effective normal tensile stress on the fault plane, and Weertman 's $\mu^*(\mathrm{v})$, dependent (like for $\bar{\mu}(\mathrm{v})$) on the different elastic properties and density on the two sides, is now augmented with the new function $W(\mathrm{v})/2$, which results from the permeability and poroelastic properties in the damaged fault border zones on the two sides. It is the functions $\mu^*(\mathrm{v})$ and $W(\mathrm{v})/2$ which can be positive or negative, and their signs generally need not agree, so that the effects can reinforce or counteract one another in different cases. Our preliminary estimates, for a 10% difference in wave speeds between the two sides and for Skempton coefficient of 0.6 in the gouge at the fault walls, suggest that $W(\mathrm{v})/2$ will generally dominate the $\mu^*(\mathrm{v})$ at low speeds, but $\mu^*(\mathrm{v})$ changes more rapidly with increase of speed and, at the generalized Rayleigh speed, will usually be comparable to, and possibly a little larger than, $W(\mathrm{v})/2$.

This adds a new twist to the bimaterial problem, much in need of exploration in spontaneous rupture simulations.

(5) Graduate student H. Noda, on a long-term visit starting in September 2005 from the Univ. of Kyoto group of T. Shimamoto, has begun, under direction of Rice and postdoc E. Dunham, to integrate weakening by thermal pressurization into the spectral BIE code for rupture dynamics. Some first results for spontaneous rupture have already been obtained. However, this work is still very preliminary, and we have not yet incorporated a suitable description of flash heating that uses concepts of the rate and state type to regularize the pure velocity weakening model. See discussion of plans for this area in the proposal.